U.S. DEPARTMENT OF ENERGY | Office of Science

DOE/SC-ARM-15-091

Analysis of the Uncertainty in Wind Measurements from the Atmospheric Radiation Measurement Doppler Lidar during XPIA: Field Campaign Report

R Newsom

March 2016

ARM
CLIMATE RESEARCH FACILITY

DISCLAIMER

This report was prepared as an account of work sponsored by the U.S. Government. Neither the United States nor any agency thereof, nor any of their employees, makes any warranty, express or implied, or assumes any legal liability or responsibility for the accuracy, completeness, or usefulness of any information, apparatus, product, or process disclosed, or represents that its use would not infringe privately owned rights. Reference herein to any specific commercial product, process, or service by trade name, trademark, manufacturer, or otherwise, does not necessarily constitute or imply its endorsement, recommendation, or favoring by the U.S. Government or any agency thereof. The views and opinions of authors expressed herein do not necessarily state or reflect those of the U.S. Government or any agency thereof.

DOE/SC-ARM-15-091

Analysis of the Uncertainty in Wind Measurements from the Atmospheric Radiation Measurement Doppler Lidar during XPIA: Field Campaign Report

R Newsom, Pacific Northwest National Laboratory
Principal Investigator

March 2016

Work supported by the U.S. Department of Energy,
Office of Science, Office of Biological and Environmental Research

Executive Summary

In March and April of 2015, the ARM Doppler lidar that was formerly operated at the Tropical Western Pacific site in Darwin, Australia (S/N 0710-08) was deployed to the Boulder Atmospheric Observatory (BAO) for the eXperimental Planetary boundary-layer Instrument Assessment (XPIA) field campaign. The goal of the XPIA field campaign was to investigate methods of using multiple Doppler lidars to obtain high-resolution three-dimensional measurements of winds and turbulence in the atmospheric boundary layer, and to characterize the uncertainties in these measurements. The ARM Doppler lidar was one of many Doppler lidar systems that participated in this study.

During XPIA the 300-m tower at the BAO site was instrumented with well-calibrated sonic anemometers at six levels. These sonic anemometers provided highly accurate reference measurements against which the lidars could be compared. Thus, the deployment of the ARM Doppler lidar during XPIA offered a rare opportunity for the ARM program to characterize the uncertainties in their lidar wind measurements.

Results of the lidar-tower comparison indicate that the lidar wind speed measurements are essentially unbiased (~1cm s^{-1}), with a random error of approximately 50 cm s^{-1}. Two methods of uncertainty estimation were tested. The first method was found to produce uncertainties that were too low. The second method produced estimates that were more accurate and better indicators of data quality. As of December 2015, the first method is being used by the ARM Doppler lidar wind value-added product (VAP). One outcome of this work will be to update this VAP to use the second method for uncertainty estimation.

Acronyms and Abbreviations

ARM	Atmospheric Radiation Measurement Climate Research Facility
BAO	Boulder Atmospheric Observatory
CABL	Characterizing the Atmospheric Boundary Layer
DOE	U.S. Department of Energy
EERE	DOE office of Energy Efficiency and Renewable Energy
ESRL	Earth Systems Research Laboratory
kHz	kilohertz
km	kilometer
lidar	light detection and ranging
LOS	line-of-sight
NCAR	National Center for Atmospheric Research
NOAA	National Oceanic and Atmospheric Administration
NSF	National Science Foundation
PNNL	Pacific Northwest National Laboratory
PPI	plan-position-indicator
PRF	pulse repetition frequency
SGP	Southern Great Plains, an ARM megasite
TWP	Tropical Western Pacific, an ARM research site
VAD	Velocity-azimuth-display
VAP	Value-Added Product
XPIA	eXperimental Planetary boundary layer Instrument Assessment

Contents

Executive Summary iii
Acronyms and Abbreviations iv
1.0 Background 1
1.1 Radial Velocity Precision 3
1.2 Wind Retrieval 3
1.3 Uncertainty Estimation 4
2.0 Lessons Learned 5
3.0 Results 5
4.0 Public Outreach 8
5.0 XPIA Publications 8
5.1 Journal Articles/Manuscripts 8
5.2 Meeting Abstracts/Presentations/Posters 8
6.0 References 9

Figures

1. Location and setup of the ARM Doppler lidar (S/N 0710-08) during XPIA 2
2. Radial velocity precision, δu_r, as a function of SNR during the XPIA deployment 3
3. Time-height cross sections for 2 April 2015 showing retrieved winds and estimated wind speed uncertainties for Method 1 and Method 2 6
4. Standard deviation of the observed difference versus estimated uncertainty from Method 2. Results for wind speed and wind direction are shown 8

Tables

1. Results of the comparison between the lidar-derived winds and the BAO measurements 7

1.0 Background

The primary goal of the eXperimental Planetary boundary-layer Instrument Assessment (XPIA) field campaign was to investigate methods of using multiple Doppler lidars to obtain high-resolution three-dimensional measurements of winds and turbulence in the atmospheric boundary layer, and to characterize the uncertainties in these measurements. The field campaign was conducted at the Boulder Atmospheric Observatory (BAO) (Kaimal and Gaynor, 1983) in March and April of 2015 with funding from the U.S. Department of Energy's (DOE) office of Energy Efficiency and Renewable Energy (EERE). The principle investigators for XPIA included Julie Lundquist from the University of Colorado, and Jim Wilczak from the National Oceanic and Atmospheric Administration (NOAA)'s Earth System Research Laboratory (ESRL). Other participants included the National Center for Atmospheric Research (NCAR), Texas Tech University, the University of Dallas, Pacific Northwest National Laboratory (PNNL), and the University of Maryland, Baltimore County.

Multiple Doppler lidar systems, including scanning and profiling systems from different manufacturers, were deployed in close proximity to the BAO's heavily instrumented 300-meter (m) meteorological tower. The BAO tower was instrumented specifically for XPIA with well-calibrated sonic anemometers at six levels. These sonic anemometers provided highly accurate reference measurements against which the lidars could be compared. The ARM Doppler lidar that was formerly deployed in Darwin Australia (S/N 0710-08) was one of several scanning Doppler lidar systems that participated in this field campaign. The deployment of ARM Doppler lidar provided the opportunity for the ARM program to exploit the unique observational capability of the 300-m BAO tower during XPIA to quantify the uncertainties in wind measurements.

The ARM Doppler lidar is a commercial-grade system manufactured by Halo Photonics Inc. in England. This instrument provides range-resolved measurements of attenuated aerosol backscatter and radial velocity, i.e., the velocity component parallel to the beam. The system employs an eye-safe laser transmitter operating at a wavelength of 1548 nm, a pulse energy of ~100 μJ and a high pulse repetition frequency of 15kilohertz (kHz). The instrument incorporates a full upper hemispheric scanner that can be configured to operate in either step-stare or continuous scan mode. The internal processor can be configured to operate using a wide range of pulse accumulation times and range gates sizes. During XPIA, the ARM Doppler lidar was operated using a range gate size of 30-m, and 200 range gates, resulting in a maximum measurement range of about 6 km. Typically, the maximum range for usable measurements varied between 1 and 3 km, depending on atmospheric conditions. Further details about the ARM Doppler lidars can be found in Pearson et al. (2009), and Newsom (2012).

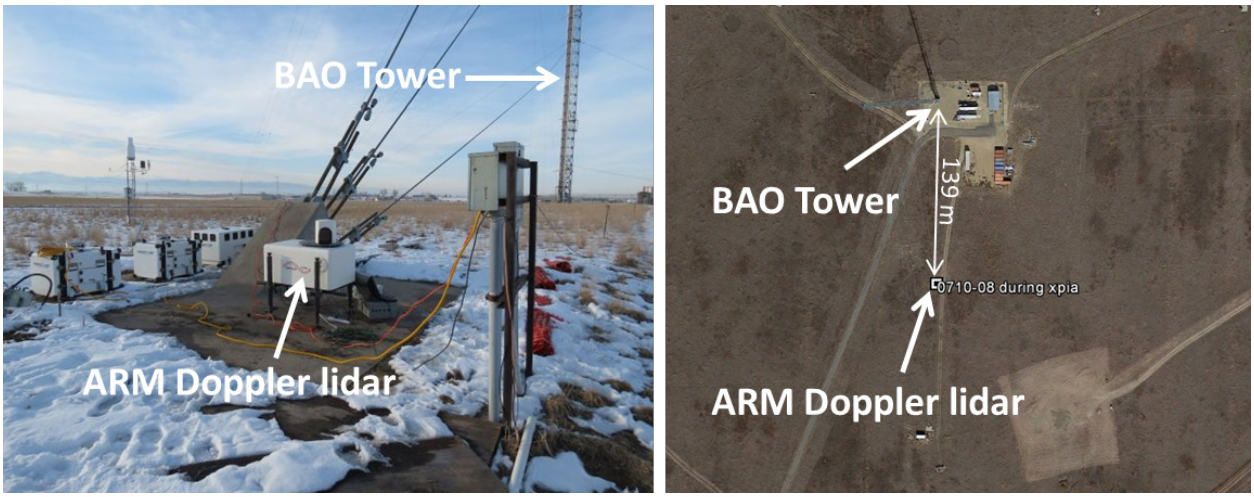

Figure 1. Location and setup of the ARM Doppler lidar (S/N 0710-08) during XPIA.

During XPIA the ARM Doppler lidar was deployed within a small cluster of profiling Doppler lidars approximately 140 m south of the BAO tower, as shown in Figure 1. The system was operated at this location from 6 March to 16 April 2015. During this time the lidar was operated using a fixed scan schedule consisting of the following:

- 40-second plan-position-indicator (PPI) scan once every 12 minutes,
- 10-minute tower stare once per hour,
- target sector scan once per day, and
- vertical stares otherwise.

The PPI scans were used to derive profiles of wind speed and direction. These scans were performed using the step-stare scan mode at an elevation angle of 60° using eight evenly spaced azimuth angles around the compass, i.e., 0°, 45°, 90°, 135°, 180°, 225°, 270°, and 315°. The pulse integration time for each line-of-sight (LOS) was set to 2 s (30000 laser pulses), and the time required to execute one complete PPI scan was about 40 seconds. The lidar was also configured to stare near the south-east sonic at the 50-m level of the BAO tower for approximately 10 minutes once per hour. Target sector scans were performed in order to accurately determine the lidar's azimuthal pointing direction relative to true north. Otherwise, the lidar stared vertically when it was not busy doing PPIs, target sector scans or tower stares.

Normally, the BAO tower is instrumented at three levels with slow-response (1Hz) temperature and wind sensors. During XPIA six additional levels (50, 100, 150, 200, 250, and 300m) of fast-response (20Hz) 3-D sonic anemometers (Campbell CSAT3) were added by NCAR. Each of these levels had two sonic anemometers, one mounted on a southeast boom (at a heading angle of 154°) and one mounted on a northwest boom (at a heading angle of 334°). This ensured that one sonic at each level was mounted on the upstream side of the tower, and thus unaffected by the tower wake. The sonic data used in this study were tilt-corrected and rotated such that "*u*" is the easterly component and "*v*" is the northerly component.

The main objective here was to characterize the uncertainty in the lidar-derived wind speed and direction as computed from the PPI scan data. Moreover, we wished to determine the accuracy of the uncertainty estimates and the extent to which the uncertainty estimates are indicators of data quality. This was

achieved by comparing the lidar-derived winds with measurements from the sonic anemometers on the tower. In the following subsection we briefly describe the method for estimating the precision of the raw radial velocity measurements. We then describe the wind retrieval and the uncertainty estimation methods.

1.1 Radial Velocity Precision

The radial velocity precision, δu_r, is an estimate of the noise variance in the radial velocity measurement. For a coherent detection system, the noise is dominated by shot noise in the photo detector. For this study, the precision was estimated from time-series analysis of vertical staring data using the technique described by Lenschow et al (2000) and Pearson et al (2009). The precision estimates were then parameterized in terms of the mean signal-to-noise ratio (SNR). Figure 2 shows the end result of this process. The blue curve in Fig. 2 was used to assign precision estimates to individual radial velocity measurements based on the corresponding SNR. When processing the lidar PPI scan data, an SNR threshold of 0.008 was imposed, as indicated by the dotted vertical line in Fig. 2. As a result, radial velocities with precisions greater than about 1ms^{-1} were not used in the processing.

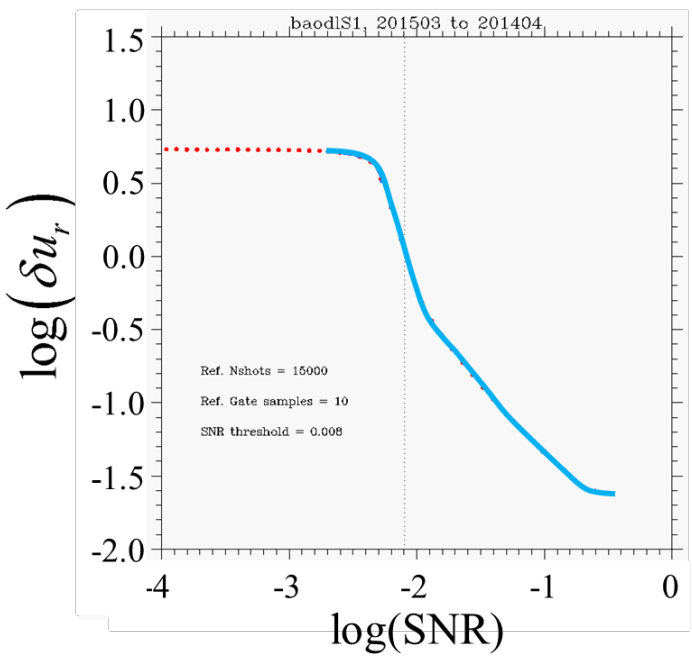

Figure 2. Radial velocity precision, δu_r, as a function of SNR during the XPIA deployment (averaged over the period 6 March to 16 April 2015).

1.2 Wind Retrieval

The wind retrieval is based on the traditional velocity-azimuth-display (VAD) approach described by Browning and Wexler (1968). The VAD algorithm estimates the velocity components of the wind field from PPI scan data. At any given height, the PPI scan traces out a circle centered above the lidar position. Assuming the flow to be horizontally uniform and steady along the circle, the wind velocity components

are retrieved by fitting a sinusoid to the radial velocity data; the amplitude, phase, and offset of the sinusoid determine the wind speed, wind direction, and vertical velocity, respectively. The derived winds are representative of averages taken over the circumference of the circle and over the time it takes to complete a full PPI scan, which in this case is about 40 s.

At a fixed-range gate, the PPI scan data are used to find the wind velocity components, *u*, *v* and *w* by minimizing the following chi-squared function:

$$\psi^2 = \sum_{i=1}^{N} \frac{\left(\mathbf{u}^T \cdot \tilde{\mathbf{r}}_i - u_{ri}\right)^2}{\sigma_i^2}, \tag{1}$$

where $\mathbf{u}$ is the unknown velocity vector, u_{ri} is a radial velocity measurement, σ_i is the measurement uncertainty, and $\tilde{\mathbf{r}}_i$ is a unit vector from the lidar to the measurement point. The summation in equation (1) is performed over all the LOSs in the PPI scan for which there are valid data at the measurement height ($N \leq 8$). Minimizing equation (1) with respect to the components of $\mathbf{u}$ (*u*, *v* and *w*) results in a system of three equations, and three unknowns, *u*, *v* and *w*. The solution is given by

$$\mathbf{u} = \mathbf{C} \cdot \mathbf{b}, \tag{2}$$

where $\mathbf{C}$ is the covariance matrix and **b** is a vector that depends on LOS direction cosines, measurement uncertainties, and the radial velocity measurements. The covariance matrix depends on the LOS direction cosines and measurement uncertainties but does not depend on the actual measurements. When the measurement uncertainties, σ_i , are known, the diagonal elements of the covariance matrix give the squared uncertainties in the components of the retrieved velocity vector.

1.3 Uncertainty Estimation

Accurate uncertainty estimation is crucial for evaluating the quality of the derived winds from the lidar. In this study, we consider two methods for estimating the uncertainty in the retrieved wind components, *u* and *v*. These two methods are described below.

- Method 1
    - Measurement uncertainty: $\sigma_i = \delta u_{ri}$
    - Retrieval uncertainty: $\sigma_u = \sqrt{C_{11}}$, $\sigma_v = \sqrt{C_{22}}$.
- Method 2
    - Measurement uncertainty: $\sigma_i = 1$

- Retrieval uncertainty: $\sigma_u = \sqrt{\frac{\psi^2}{(N-3)} C_{11}}$ and $\sigma_v = \sqrt{\frac{\psi^2}{(N-3)} C_{22}}$

In Method 1 the radial velocity precisions, δu_{ri}, are used as the measurement uncertainties, σ_i, and the uncertainties in the retrieved parameters, *u* and *v*, are obtained from the diagonal elements of the weighted covariance matrix (Press et al. 1988). In Method 2, the measurement uncertainty is assumed to be unknown, and the uncertainties in *u* and *v* are estimated by scaling the unweighted covariance matrix with ψ^2. This approach assumes a good fit and precludes an independent estimate of the goodness of fit (Press et al. 1988).

Given the uncertainties in *u* and *v* from either method, the estimated uncertainty in the retrieved wind speed is given by

$$\sigma_M^{est} = \left((u\sigma_u)^2 + (v\sigma_v)^2 \right)^{1/2} / M \tag{3}$$

where M is the lidar wind speed, $M = \sqrt{u^2 + v^2}$, and the estimated wind direction uncertainty is given by

$$\sigma_\alpha^{est} = \left((u\sigma_v)^2 + (v\sigma_u)^2 \right)^{1/2} / M^2 . \tag{4}$$

2.0 Lessons Learned

The deployment of the ARM Doppler lidar to the BAO during XPIA afforded a valuable opportunity to characterize the uncertainties in the lidar wind measurements against well-calibrated in situ measurements on the 300-m BAO tower. One lesson learned from this deployment is that the lidar wind speed measurements are essentially unbiased (~1cm s^{-1}), with a random error of approximately 50 cm s^{-1}, based on direct comparisons with the BAO tower. More importantly, it was found that Methods 1 and 2, as described in Section 1.3, result in substantially different estimates of the random error. Method 2 gave superior results, and provided more accurate uncertainty estimates than Method 1. Currently (as of December 2015), Method 1 is being used by the ARM Doppler lidar wind value-added product (VAP). One outcome of this effort will be to update this VAP to use Method 2 for uncertainty estimation.

3.0 Results

Figure 3 shows representative lidar wind retrieval results for 2 April 2015. The results using Method 1 are shown in panel (a) and the results using Method 2 are shown in panel (b). The retrieved wind speed and direction for the two methods look qualitatively similar; however, the uncertainty estimates are radically different in both magnitude and structure. The uncertainty estimates for Method 1 are much smaller than for Method 2. We also notice that the uncertainty estimates from Method 2 tend to follow the variability in the flow, whereas the uncertainty estimates from Method 1 vary with the SNR and are largely independent of the flow variability.

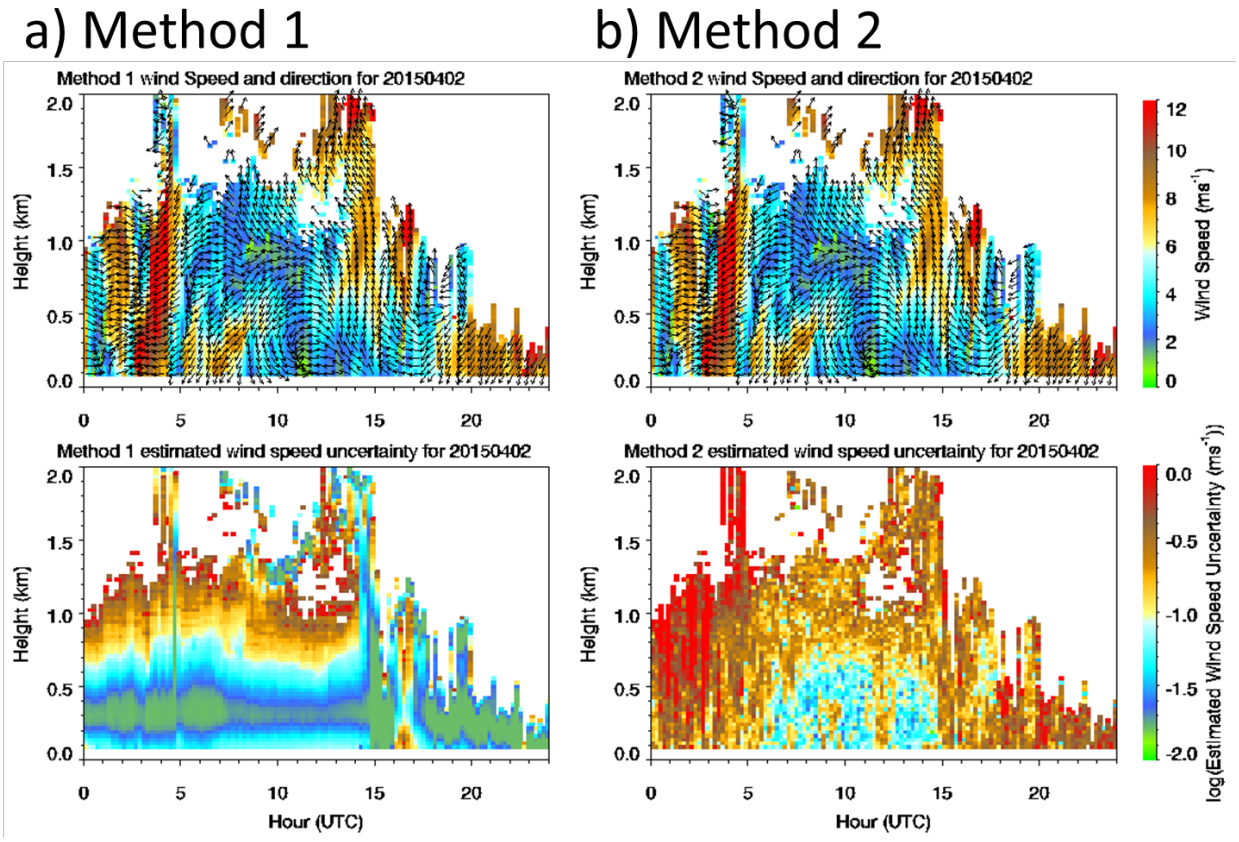

Figure 3. Time-height cross sections for 2 April 2015 showing retrieved winds (top) and estimated wind speed uncertainties (bottom) for a) Method 1 and b) Method 2.

To enable comparison with the lidar-derived winds, 20Hz *u* and *v* data from each sonic anemometer were averaged in time and then interpolated to the heights of selected lidar range gates. The center times of the averaging intervals were set to the center times of the PPI scans, and the averaging intervals were set equal to twice the PPI scan durations, i.e. ,nominally 80s. The temporally averaged *u* and *v* data were then interpolated to the heights of those lidar range gates with heights closest to the anemometer heights. This helped to minimize the effects of the vertical interpolation on the final results. The lidar heights that occur closest to the sonic heights were 90.9, 142.9, 194.9, 246.8, and 298.8 m. Also, to minimize the effects of tower flow distortion on the results, only those anemometers on the upstream side of the tower were used in the comparison.

The comparison is carried out by computing statistics of the wind speed difference

$$\Delta_M = M - M_s \,, \tag{5}$$

and the wind direction difference,

$$\Delta_\alpha = \tan^{-1}\left(\frac{\sin\alpha\cos\alpha_s - \cos\alpha\sin\alpha_s}{\sin\alpha\sin\alpha_s + \cos\alpha\cos\alpha_s}\right), \tag{6}$$

where $\alpha = \tan^{-1}(u/v)$ is the azimuth angle of the horizontal velocity vector from the lidar, M_s is the sonic wind speed, and α_s is the azimuth angle of the horizontal velocity vector from the sonic. The wind direction difference Δ_s is positive when the lidar winds are rotated clockwise relative to the sonic winds.

Table 1 summarizes the results of the comparison between the lidar and sonic winds using Methods 1 and 2. The wind speed bias is denoted by $\overline{\Delta_M}$ and the standard deviation of the wind speed difference is denoted by $\sigma(\Delta_M)$. Similarly, the wind direction bias is denoted by $\overline{\Delta_\alpha}$ and the standard deviation of the wind direction difference is denoted by $\sigma(\Delta_\alpha)$.Also shown is the Pearson correlation coefficient, r_{wspd}, between the sonic and lidar wind speeds, and the slope and offset (i.e., intercept) of the linear regression between the sonic and lidar wind speeds. These results represent averages taken over five height levels (90.9, 142.9, 194.9, 246.8, and 298.8 m) and over the entire deployment period from 6 March through 16 April, 2015.

Table 1. Results of the comparison between the lidar-derived winds and the BAO measurements.

Rejection Rate	**0%**		**50%**	
Method	**1**	**2**	**1**	**2**
$\overline{\Delta_M}$ (ms^{-1})	-0.04	-0.01	-0.01	-0.01
$\sigma(\Delta_M)$ (ms^{-1})	0.85	0.73	0.78	0.35
r_{wspd}	0.965	0.973	0.971	0.992
Regression offset (ms^{-1})	0.192	0.120	0.103	0.040
Regression Slope	0.967	0.976	0.980	0.993
$\overline{\Delta_\alpha}$ (deg)	-0.84	-0.74	-0.79	-0.64
$\sigma(\Delta_\alpha)$ (deg)	20.02	18.68	19.18	8.72

Tests were performed to examine the effect of imposing different σ_M thresholds on the statistics. Table 1 shows the results using two different wind speed uncertainty (σ_M) thresholds. The thresholds are defined by the so-called data rejection rates of 0% and 50%. A 0% rejection rate corresponds to no data rejection, and thus no threshold. A 50% rejection rate corresponds to rejection of all wind speed and direction estimates with σ_M greater than its median value.

It is clear from Table 1 that Method 2 outperforms Method 1 in terms of all the statistical metrics considered, regardless of the data rejection rate. Although the wind speed biases are quite small for either method, Method 2 produces substantially better agreement with the tower sonics in terms of random errors, linear regressions, and correlations. Moreover, the results for Method 2 exhibit better improvement as the σ_M threshold is lowered. This indicates that the uncertainty estimates produced by Method 2 are more reliable indicators of data quality.

The uncertainty estimates (σ_M^{est} and σ_α^{est}) produced by Method 1 tend to grossly underestimate the observed uncertainties ($\sigma(\Delta_M)$ and $\sigma(\Delta_\alpha)$). Although Method 2 does a much better job, it also tends to underestimate the observed uncertainties somewhat. Figure 4a shows the observed versus estimated wind speed uncertainty for Method 2, and Figure 4b shows the observed versus estimated wind direction uncertainty. The curves indicate approximately linear relationships between the observed and estimated uncertainties.

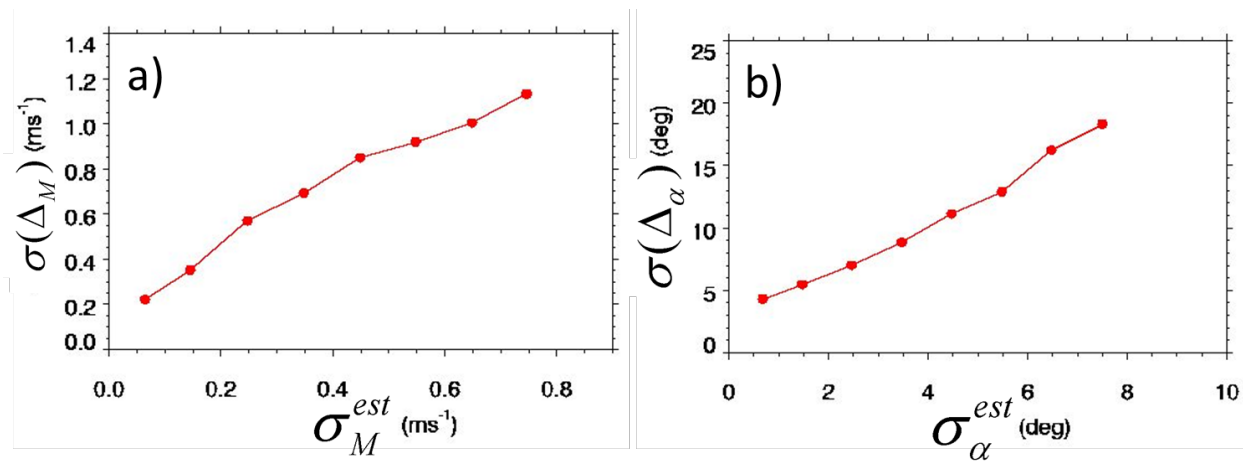

Figure 4. Standard deviation of the observed difference versus estimated uncertainty from Method 2. Results for a) wind speed and b) wind direction are shown.

4.0 Public Outreach

The XPIA field campaign leveraged support from the "Characterizing the Atmospheric Boundary Layer" (CABL) educational outreach project (http://www.eol.ucar.edu/field_projects/cabl). This NSF-funded project created learning opportunities for high school, undergraduate, and graduate students in Colorado's Front Range. CABL also helped supplement instrument deployments during XPIA.

5.0 XPIA Publications

5.1 Journal Articles/Manuscripts

Lundquist JK, et al. 2015. "Assessing state-of-the-art capabilities for probing the atmospheric boundary layer: The XPIA field campaign." To be submitted to BAMS.

Lundquist JK, et al. 2015. The XPIA field campaign. DOE Technical Report, to be submitted.

5.2 Meeting Abstracts/Presentations/Posters

Brewer WA, et al. 2015. Initial Results from the Experimental Measurement Campaign for Planetary Boundary layer (PBL) Instrument Assessment (XPIA) Experiment. 27th International Laser Radar Conference, New York, NY, July 5-10, 2015.

6.0 References

Browning, K and R Wexler. 1968. "The determination of kinematic properties of a wind field using Doppler radar." *Journal of Applied Meteorology* 7: 105-113, doi:10.1175/1520-0450(1968)007-0105:TDOKPO>2.0.CO;2.

Kaimal, JC and JE Gaynor. 1983. "The Boulder Atmospheric Observatory." *Journal of Climate and Applied Meteorology* 22: 863-880.

Lenschow, DH, V Wulfmeyer, and C Senff. 2000. "Measuring second- through fourth-order moments in noisy data." *Journal of Atmospheric and Oceanic Technology* 17: 1330-1347, doi:10.1175/1520-0426(2000)017<1330:MSTFOM>2.0.CO;2.

Newsom, RK. 2012. Doppler Lidar Handbook. DOE/SC-ARM-TR-101.

Pearson, G, F Davies, and C Collier. 2009. "An analysis of the performance of the UFAM pulsed Doppler lidar for observing the boundary layer." *Journal of Atmospheric and Oceanic Technology* 26: 240-250, doi:10.1175/2008JTECHA1128.1.

Press, WH, BP Flannery, SA Teukolsky, and WT Vetterling. 1988. *Numerical Recipes in C*. Cambridge University Press, Cambridge, pp. 528-534.

ARM

CLIMATE RESEARCH FACILITY

www.arm.gov

U.S. DEPARTMENT OF ENERGY

Office of Science